Molecular Dynamics Simulations of $Na_2Si_4O_9$ Liquid at High Pressure

Jason Diefenbacher*

Science & Engineering of Materials Program, Arizona State University, Tempe, Arizona 85287-1704

Paul F. McMillan

Center for Solid State Science, Arizona State University, Tempe, Arizona 85287-1704, and Department of Chemistry & Biochemistry, Arizona State University, Tempe, Arizona 85287-1604

George H. Wolf

Department of Chemistry & Biochemistry, Arizona State University, Tempe, Arizona 85287-1604

Received: October 8, 1997; In Final Form: February 18, 1998

Molecular dynamics (MD) simulations are used to investigate the structural and transport properties of $Na_2Si_4O_9$ liquid as a function of pressure. Simulations were performed at 6000 K at a variety of pressures, ranging from 1 atm to 100 GPa. The calculated oxygen self-diffusivity increases with increasing pressure, up to approximately 10−15 GPa, as found in previous simulations and experimental studies. Above this pressure, the O^{2-} diffusivity decreases slightly with increasing pressure. From the MD results, we distinguish two distinct mechanisms for the pressure-induced coordination change of silicon. The first, occurring in the lower pressure regime, below 15 GPa, involves formation of $^{[5]}$Si species via a reaction with the nonbridging oxygen atoms. The second mechanism occurs at high pressures via a reaction of the bridging oxygen atoms and results in the formation of $^{[3]}$O species.

Introduction

There has been much recent interest in understanding the structural changes in glassy materials, particularly silicate glasses, at high pressures,[1] and also in the inter-relationships between structure and rheological properties in the high-temperature liquids, particularly as the glass transition is approached.[2−4] Of particular interest is the interplay between the structure and dynamics in the glass-forming liquids at high pressures, in a regime where anomalous viscosity *decreases* are observed with increasing density.[1,5−9] This problem is of importance in geochemistry, for understanding the behavior of molten silicate materials at depth.[7−11]

Several recent experimental and computer simulation studies have focused on the behavior of simple silicate glasses and melts at high pressure.[4,12,13] Several classes of study can be distinguished: (i) studies at ambient conditions of glasses quenched from melts prepared at high pressure and temperature, (ii) in situ studies of glasses at room temperature and high pressure, and (iii) a few exploratory studies of glasses and supercooled liquids under combined high-$P-T$ conditions. Computer simulations are not subject to the same experimental constraints as laboratory studies, and much of our present understanding of the atomic-level structure and dynamics in high-pressure melts has been obtained from computer studies (primarily molecular dynamics simulations). In the present work, we have used the molecular dynamics technique to investigate the structural changes during densification and associated changes in transport properties in a model silicate melt ($Na_2Si_4O_9$ composition) to complement previous experimental studies on melts and quenched glasses.

* Corresponding author: Fax (602) 965-0474; E-mail Jason.Diefenbacher@asu.edu.

Xue et al.[13] prepared samples of $Na_2Si_4O_9$ and $K_2Si_4O_9$ glasses at pressures up to 12 GPa and studied the changes in Si coordination in the recovered samples via NMR spectroscopy. In previous work, high-coordinate (5- and 6-fold coordinated) silicate species had been identified in alkali silicate glasses synthesized at high pressure and decompressed to ambient conditions.[13,14] Xue et al.[13] found that the proportion of $^{[5]}$Si and $^{[6]}$Si species increased with increasing quench pressure, to values of 8% $^{[5]}$Si and 6% $^{[6]}$Si for $Na_2Si_4O_9$ glass synthesized at 12 GPa. Formation of these high-coordinate species provides an important densification mechanism for the silicate glass.[1,12,13] Parallel studies on silicate melts, supercooled liquids, and glasses at room pressure had indicated that the $^{[5]}$Si species also appears to play an important role in the mechanism for O^{2-} transfer between adjacent silicate polymer units and hence in oxygen diffusion and viscous relaxation in the melt.[15,16] These processes are of critical importance in determining viscous slowdown as the glass transition is approached.[17]

Wolf et al.[12] studied structural changes in $Na_2Si_4O_9$ glass (at room temperature) in situ at high pressure using Raman spectroscopy. It was found that the dominant high-frequency band, which arises from the symmetric $Si-O^-$ stretching of Q^3 tetrahedral silicate units, had disappeared by approximately 20 GPa. These authors proposed that, during compression, the "nonbridging" oxygen atoms ($^{[1]}$O species) form new Si−O−Si linkages with adjacent (tetrahedral) silicon atoms, resulting in formation of $^{[5]}$Si species.[12,13] This would provide an efficient densification mechanism for pressures up to 20 GPa, where the $^{[1]}$O species are almost entirely consumed. Continued compression above 20 GPa resulted in broadening of the low-frequency band manifold (assigned to SiOSi bending vibrations) accompanied by a shift to higher wavenumber, changes which

S1089-5647(97)03276-8 CCC: $15.00
Published on Web 03/31/1998

TABLE 1: Born−Mayer Parameters Used in These Simulations

				b_{ij} ($\times 10^{-9}$ erg m^{-1})		
species	mass (amu)	z_i	σ (Å)	Na	Si	O
Na	22.9900	+1	0.1252	2.375	2.898	1.595
Si	28.0855	+4	0.1310	2.898	3.420	2.117
O	15.9994	−2	0.1420	1.595	2.117	0.814

were interpreted to indicate that further increase in the average Si coordination occurred through the involvement of *bridging* oxygens, to form $^{[3]}$O species. In the present study, we have used molecular dynamics (MD) simulations to examine the densification mechanisms in molten $Na_2Si_4O_9$ at high pressure and to correlate the structural changes with transport properties of the densified melt.

MD simulations have been used extensively to study the structures and dynamics of silicate liquids and glasses at ambient and at high pressure.[16,18,19] In their pioneering MD study of SiO_2 liquid, Woodcock et al.[20] first noted an unusual effect: that increasing pressure resulted in an *increase* in the Si^{4+} and O^{2-} diffusivities, to reach maximum values near 20 GPa. This anomalous behavior could be associated with an increased abundance of $^{[5]}$Si species in the liquid at high pressure.[19,21] Later investigations showed similar behavior in the simulated liquids $CaMgSi_2O_6$, $NaAlSi_2O_6$, and $Na_2Si_3O_7$.[5,6,22]

Rubie et al.[23] and Poe et al.[24] have recently measured the self-diffusion constants of O^{2-} and Si^{4+} as a function of pressure for $Na_2Si_4O_9$ liquid. In general agreement with the results of the MD studies, the O^{2-} and Si^{4+} diffusivities were found to increase with increasing pressure.

In the present MD simulations, we studied Na^+, Si^{4+}, and O^{2-} self-diffusivities in $Na_2Si_4O_9$ liquid to a pressure of 70 GPa. The diffusivities compare well with available experimental data and have been used to estimate the viscosity of the liquid as a function of pressure. The results of the simulations also give a detailed picture of structural changes occurring within the liquid at high pressure, which provides a framework for understanding the change in transport properties.

Details of Simulations

The MD simulations were carried out using a rigid-ion Born−Mayer−Huggins pair potential to model the interparticle interactions. In this model, the potential between ions *i* and *j* depends only on their separation, *r*, and is given (in cgs units) by

$$U_{ij}(r) = \frac{e^2 z_i z_j}{r} + b_{ij} \exp\left[\frac{\sigma_i + \sigma_j - r}{\rho}\right] \qquad (1)$$

The first term is the point-Coulomb interaction, where z_i and z_j are the full formal charges of the ions. The second term is the short-range repulsion interactions, with potential parameters listed in Table 1. This parameter set has been developed over several years in Angell's group.[5,6,20] The original Si and O parameters for SiO_2 were chosen for their ability to reproduce the first diffraction peaks in the glassy radial distribution function.[20]

The molecular dynamics simulations were carried out in a cubic box of fixed volume using periodic boundary conditions. Each simulation was independently started from a random configuration which was initially run at 8000 K for 5000 time steps (each time step was 2 fs) to ensure proper mixing of particles. Most calculations used $N = 345$ particles, which permitted a large number of simulations to be performed within the capabilities of our available computational resources (a Silicon Graphics Indy, R4000 SC at 100 MHz). The effect of system size on calculated properties can be important in such calculations[16,18,25] and is addressed in the Appendix. Following the initial mixing period, the system was then cooled to the working temperature of 6000 K and maintained in the canonical NVT ensemble for at least 20 000 time steps in order to fully equilibrate the system before being run for the mean-square displacement calculations. In some instances, longer equilibration run times were necessary for the model to completely relax from the initial configuration state. In the NVT ensemble, the pressure was obtained from the average virial.

Mean-square displacement averages were obtained for a minimum of 50 000 time steps (100 ps). Over this time interval, the particles diffuse, on average, a minimum distance equal to the length of a box side. Linear least-squares fits were performed on the mean-squared displacement plots to determine the ionic diffusivities (D_i), obtained using Einstein's equation:

$$D_i = \langle (u_i)^2 \rangle / 6t \qquad (2)$$

The subscript i labels the ionic species, and u_i is the total displacement of a particular ion over the time interval, *t*. In all cases, the mean-squared displacements were plotted before the data were fit to ensure that a linear behavior representing true liquidlike diffusion was present, rather than the ballistic trajectories which can appear in the onset of simulations.[16] For this reason, the initial 500 steps of each run were not typically used in the calculation of the diffusion profiles.

Melt viscosities (η) were calculated from the O^{2-} diffusivity using the Stokes−Einstein relation:

$$\eta = \frac{k_B T}{6\pi\lambda D_{O^{2-}}} \qquad (3)$$

where *T* is the absolute temperature, k_B is Boltzmann's constant, and λ is an appropriate atomic jump distance, taken to be 2.5 Å for O^{2-} diffusion.[26] This equation is found to be most appropriate for relating viscosity and diffusivity in highly fluid systems, in which the diffusive motion of the particle in question is well coupled to the viscous relaxation of its environment.[6,26]

Results and Discussion

Equation of State. The pressure−volume (*P*−*V*) equation of state of the model liquid at 6000 K was obtained from a series of simulations carried out in the canonical (NVT) ensemble and is shown in Figure 1. The calculated results were fit to a third-order Birch−Murnaghan equation,[27] yielding values for the bulk modulus, $K_o = 7.5$ GPa, and its pressure derivative, $K' = 9.25$. These values of K_o and K' appear quite reasonable for sodium tetrasilicate liquid,[28] based on available compositional systematics for melt compressibilities. Using the empirical method proposed by Lange and Carmichael,[29] we estimate a bulk modulus of approximately 13.7 GPa for this composition at 6000 K.

In the low-pressure regime, the pressure density equation of state of the simulated liquid approaches zero slope and hence a diverging compressibility for densities below 2.5 g/cm^3 (Figure 1), indicating the onset of an impending volume instability (spinodal) in the liquid at slightly negative pressures. This behavior could be of some geochemical relevance, because rapid decompression of magmas during explosive silicic volcanism (with decompression rates on the order of 40 MPa m/s[30]) might place the liquid under such tensile stress. The structural

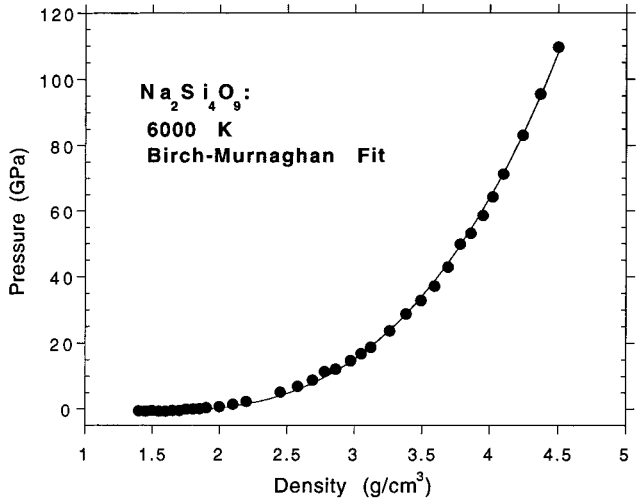

Figure 1. Pressure−density plot for $Na_2Si_4O_9$ liquid at 6000 K. Simulations were performed in the canonical (NVT) ensemble, with the pressure obtained by the virial. The solid line represents the third-order Birch−Murnaghan fit, $K_o = 7.5$ GPa and $K_o' = 9.25$.

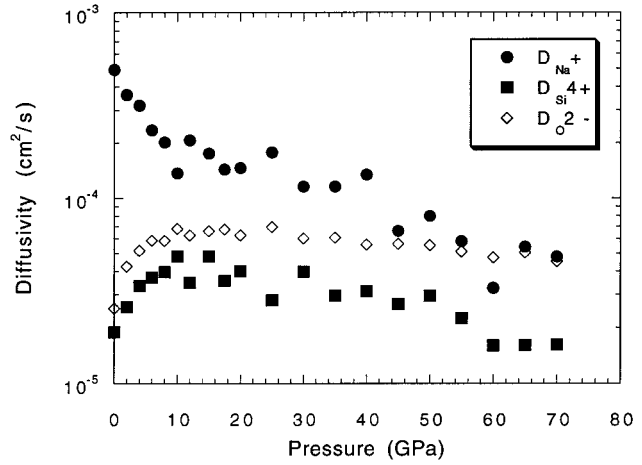

Figure 2. Calculated self-diffusion coefficients for Na^+, Si^{4+}, and O^{2-} ions in $Na_2Si_4O_9$ liquid at 6000 K as a function of pressure. A rapid decrease in diffusivity with pressure is evident for sodium, while the network ions, Si^{4+} and O^{2-}, display an initial increase in diffusivity with increasing pressure, passing through a maximum between 10 and 20 GPa.

instability associated with the spinodal limit could then contribute to the observed fracturing and fragmentation of the erupting magma.[30]

Transport Properties. The calculated self-diffusion constants, D_i, for Na^+, Si^{4+}, and O^{2-} in the model $Na_2Si_4O_9$ liquid at 6000 K as a function of pressure are plotted in Figure 2. The sodium ion undergoes a monotonic decrease in diffusivity as pressure increases, as is expected for a non-network-forming ion diffusing via a "rattle and hop" mechanism.[6,22] At low pressures, the oxygen and silicon diffusivities increase with increasing pressure, consistent with the results of previous simulations and experimental studies.[5,6,22,23] Between 10 and 20 GPa, the self-diffusion constants of these ions reach a maximum, to values about 5 times larger than those at ambient pressure. At higher pressure, the O^{2-} diffusion remains approximately constant (or shows a slight decrease) whereas the Si^{4+} diffusivity shows a more pronounced decrease with increasing pressure. At 60 GPa, the Si^{4+} diffusion coefficient is less than its ambient-pressure value, while the self-diffusion constant for O^{2-} at 60 GPa remains greater than its value at ambient pressure.

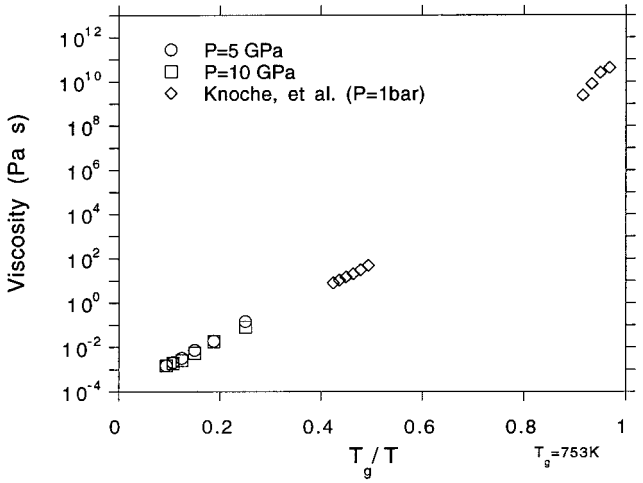

Figure 3. Logarithm of the viscosity (in Pa s) of $Na_2Si_4O_9$ liquid as a function of T/T_g. Experimental data[36] are taken at 1 atm. Simulation results at 5 and 10 GPa are estimated from the oxygen self-diffusion constants using the Stokes−Einstein relation.

The simulation results are generally consistent with experimental data. Measurements have found that the oxygen diffusivity in liquid $Na_2Si_4O_9$ increases with pressure up to at least 15 GPa, the maximum pressure to which $D_{O^{2-}}$ has been measured for this system to date.[23,24] A maximum in the pressure dependency of $D_{O^{2-}}$ cannot be resolved in the available experimental data. At 15 GPa and 2500 K the measured oxygen diffusivity is about 8−10 times larger than its value at ambient pressure for the same temperature. Although this change is larger than that found for the simulation results, this discrepancy could result from the difference in temperature between experimental (2000−2800 K) and simulation (6000 K).

We have used our simulated $D_{O^{2-}}$ values to estimate the viscosity of $Na_2Si_4O_9$ liquid at 6000 K as a function of pressure via the Stokes−Einstein relation. The initial increase in O^{2-} diffusivity results in a decrease in η of nearly 0.2 log units between ambient pressure and 10 GPa. At 60 GPa the calculated viscosity is still lower than the value at ambient pressure.

We have also investigated the temperature dependence of the viscosity from simulations at 5 and 10 GPa for temperatures between 6000 and 3000 K. The calculated viscosities (log η, in Pa s) are plotted versus T_g/T (where T_g is taken to be 753 K, the experimental glass transition temperature at ambient pressure) in Figure 3, compared with experimental values obtained at 1 bar. The calculated viscosities of the simulated liquid fall on a high-T VTF extrapolation of the experimental log η (T_g/T) relation. It is expected that the glass transition temperature will likely not change much with increasing pressure, certainly not enough to change the data as presented in Figure 3.

Melt Structure. The melt structure was examined as a function of pressure to observe any structural changes that could be correlated with the transport properties. Figure 4 shows a typical probability function $g(r)$ of finding O^{2-} ions at a distance r from any particular Si^{4+} ion. The cutoff distance for determining the coordination of one ion about the other is taken as the minimum after the first peak in the radial distribution function, as indicated by the arrow. The coordination numbers are calculated using this distance as the radial cutoff of the first coordination sphere of the ion and integrating over the representative sample for approximately 1000 time steps.

At ambient pressure, the liquid consists predominantly of 4-coordinated Si species with a small proportion (<15%) of

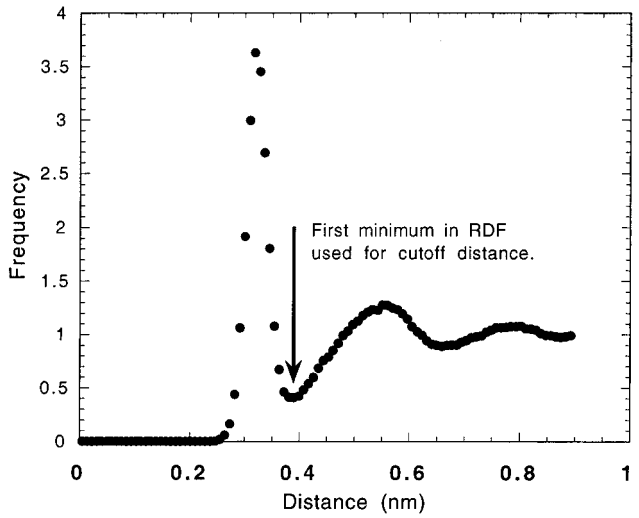

Figure 4. Typical reduced radial distribution function $g_{Si-O}(r)$. The arrow indicates the minimum after the first peak, which is taken as the cutoff distance for the first coordination sphere.

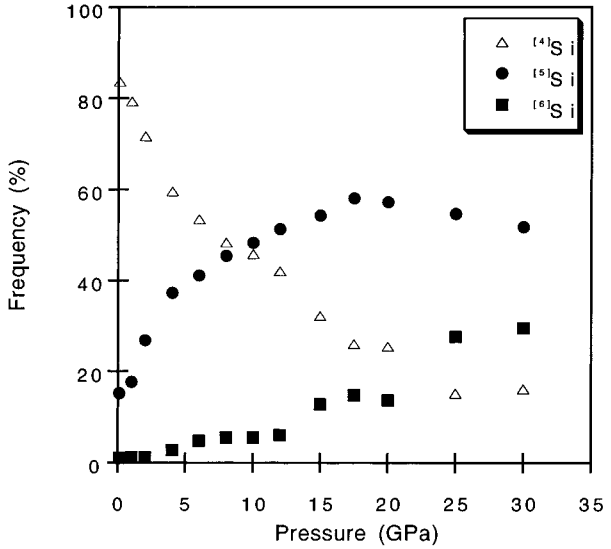

Figure 5. Pressure dependence of the Si coordination distribution (by oxygen). Mainly 4-coordinated at low pressure, the liquid quickly begins a rapid tradeoff between 4- and 5-coordinated species as the liquid is compressed. Only a small amount of transient 6-coordinated Si exists, until above 15 GPa, where the amount of 5-coordinated Si is stabilized at ~60% and the 6-coordinated species begins to increase, at the expense of the 4-coordinated Si.

5-coordinate Si species and essentially no (<1%) [6]Si. With increasing pressure, the average silicon coordination (Figure 5) increases steadily. Up to about 15 GPa, this change mainly occurs through an increase in the relative abundance of [5]Si species and a concomitant decrease in [4]Si. At 10 GPa, the relative abundances of the [4]Si and [5]Si species are approximately equal. Although there is also a small increase in the proportion of [6]Si species in the melt with increasing pressure, its abundance remains below 5% up to nearly 15 GPa. Above 15 GPa, the abundance of [5]Si begins to level off and drop while the concentration of [4]Si species continues to decrease. Also, beginning between 12 and 15 GPa, there is an abrupt increase in the pressure dependence of the [6]Si fraction. At 30 GPa, six-coordinate silicon represents nearly 30% of the silicon species in the melt.

The intermediate-range structure of the melt can be partly described by the distribution of the so-called silicon tetrahedral Q^n species, where $(4 - n)$ is the number of oxygen atoms in the tetrahedral unit that are not bonded to another silicon atom, i.e., *nonbridging* oxygen (*nbo*) atoms. At ambient pressure, spectroscopic measurements have found that the liquid contains an approximately equal number of Q^3 and Q^4 species near the glass transition temperature. For this distribution, the liquid consists of 78% 2-coordinated oxygen and 22% 1-coordinate oxygen (i.e., nbo's). This distribution of oxygen species is approximately observed for the simulated liquid at 6000 K.

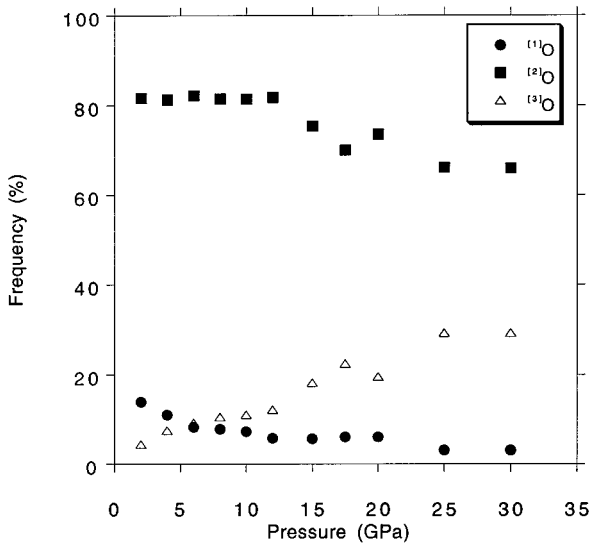

Figure 6. Pressure dependence of oxygen coordination distribution (by silicon).

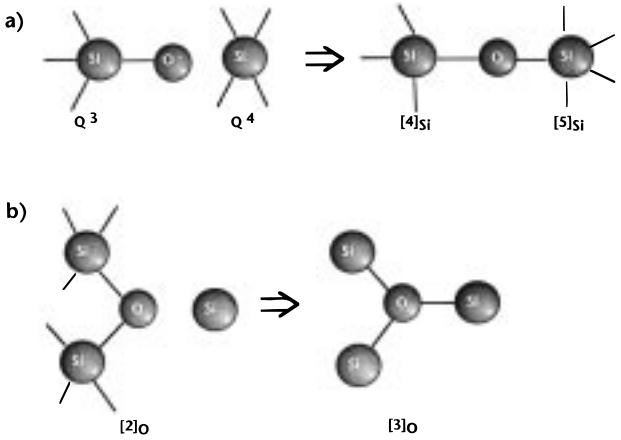

Figure 7. Diagram of proposed compression mechanism for partially depolymerized silicate liquid. (a) Initial compression mechanism, forming the 5-coordinated species. (b) Higher pressure compression mechanism which takes place above 15 GPa. Formation of higher coordination species through the use of a bridging oxygen.

The pressure dependence of the oxygen coordination is shown in Figure 6. In the low-pressure regime, below 12 GPa, there is a large reduction in the concentration of [1]O nbo species with increasing pressure and essentially no change in the [2]O concentration. At 12 GPa the relative abundance of the nbo species is reduced to about 6%. Beginning at about 12 GPa, there is a marked decrease in the relative abundance of [2]O species with increasing pressure. This is consistent with the model proposed by Wolf et al.,[12] who suggested that the mechanism depicted in Figure 7a continues until all nbo's (Q^3 species) are used up. Further compression then requires a densification mechanism involving the bridging oxygens (Figure 7b).

Previous MD simulations on silicate and fluoroberyllate liquids have highlighted the relationship between network anion (O^{2-}, F^-) diffusivity and the concentration of $^{[5]}$Si or $^{[5]}$Be species.[31] Stebbins[32] showed that formation of $^{[5]}$Si in alkali tetrasilicate melts is endothermic, with $\Delta H_f^o \sim 20$ kJ/mol. Formation of these species by the reaction described above provides a mechanism for O^{2-} transfer between adjacent silicate units[1,12,13,16,33] and also for shear relaxation in the melt.[34,35] The same factors responsible for increasing the proportion of the $^{[5]}$Si species by densification, i.e., bringing the nbo closer to an adjacent Si^{4+} and lengthening and weakening the Si−O bonds, will lower the activation energy for the O^{2-} transfer reaction and for Si−O bond breaking and re-formation. This then increases the diffusivity and lowers the viscosity. The viscosity is also lowered through the increased configurational entropy associated with the greater number of silicate species involved in the relaxational channels.

Conclusions

The results of these molecular dynamics simulations give important insights into the high-pressure behavior of the $Na_2Si_4O_9$ melt. From the simulations, we predict that the O^{2-} and Si^{4+} diffusivity increase (and viscosity decrease) observed in the laboratory should slow down and pass through a maximum (or minimum) at higher pressure, and the O^{2-} and Si^{4+} diffusivities should become increasingly decoupled. The viscosity will remain lower than the ambient pressure value to at least 70 GPa. The results of this study have also proved useful in distinguishing the mechanism of densification in $Na_2Si_4O_9$ liquid and correlating this with the transport properties as well as giving supportive evidence for the occurrence of two densification mechanisms with increasing pressure previously proposed on the basis of experimental observations,[12,13] based on the observation of high-coordinate silicon and oxygen species in the high-pressure melt. The formation of $^{[5]}$Si species via the reaction with nonbridging oxygen atoms at low pressures forms the first densification mechanism, while the second mechanism involves the reaction of bridging oxygens, resulting in the fomation of $^{[3]}$O species.

The behavior of the liquid in the tensile (negative pressure) regime suggests the approach of an impending spinodal limit in the simulated silicate melt, during which rapid changes in liquid volume occur in response to very small changes in pressure, coupled with a rapid increase in the energy of the liquid. The instabilities in this region may be indicative of conditions similar, on a local scale, to the conditions that lead to spontaneous fragmentation of magma samples under rapid decompression.[30]

Appendix

Simulation Size Dependence of Transport Properties. Simulation studies of silicate melts have indicated that close attention must be paid to the size (i.e., number of particles) of the model system and that it is essential to ascertain any size dependency in the calculated properties. In a previous MD study of SiO_2, Rustad et al.[25] found that for small numbers of particles (<252) the mean-squared displacement ($\langle u^2 \rangle$) versus time curves did not converge to a well-defined slope, and the system therefore had not reached equilibrium. They further suggested that the amplitude of the diffusivity maximum observed with increasing pressure decreases and shifts to lower pressures as the system size increases. These authors suggested that a system size of 864 particles was sufficient to determine the diffusion behavior of SiO_2 under high pressure but that smaller numbers were sufficient at lower pressures. However, it should be noted that several of the MSD curves upon which Rustad et al. based these statements were not linear with time but were parabolic in nature. This indicates a net center-of-mass momentum for the primary cell or that the diffusive regime being examined was not well-defined.[16] It is probable that cell momentum effects would exhibit themselves more readily for systems with fewer particles.

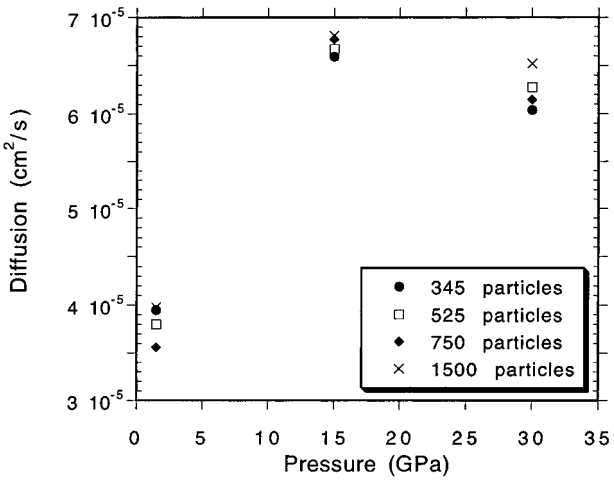

Figure 8. Plot of calculated oxygen diffusion coefficients for $Na_2Si_4O_9$ liquid versus pressure for varying numbers of particles used in the simulation. Data for differing simulations sizes agree to within ±10%. Notice that there is no systematic trend of diffusivity with number of particles and that the general trend across the pressure range is also reproduced.

Stein and Spera[18] also studied the effect of variations in the reciprocal space cutoff for the Ewald sum in reducing the error in calculation of these properties and suggested that calculations done with 400−600 particles might not be adequate to accurately calculate transport properties of the melt.

Stein and Spera[18] cited the results of Rustad et al.[25] to suggest that, for system sizes with less than ≈1300 particles, the mean-square displacements do not give a linear $\langle u^2 \rangle(t)$ relation in the long time limit and that, consequently the self-diffusion constant cannot be uniquely determined. These authors also noted an increase in instantaneous temperature fluctuations with smaller system size and larger variations in the calculated self-diffusivities for both smaller number of particles and a reduced spatial resolution. Specifically, these authors claimed that the self-diffusion constant may vary by as much as 100% when too few particles are used.[18]

To investigate the effect of system size, in our study, simulations were carried out at pressures of 2, 15, and 30 GPa, with system sizes (N) ranging from 345 to 1500 particles. The calculated oxygen diffusion coefficients are plotted in Figure 8. The diffusivities calculated at each pressure agree to within 5−10%. In view of the run-to-run imprecision in obtaining these parameters, as well as in determining pressure in the NVT ensembles, this variation is not significant, particularly as the diffusivities change by a factor of 2 over this pressure range. In general, the largest system size did tend to give the highest values of D; however, there is not a reliable systematic relation between D and N, due to run-to-run variability (Figure 8). Most importantly for the present study, the trend of variation in diffusivities with pressure is independent of the number of particles used, for N between 345 and 1500 particles. Although the use of larger systems does give rise to smaller temperature and pressure fluctuations throughout the simulation, which improves the precision and accuracy of simulated properties,[18]

due to the large number of runs in our study, it was only feasible to carry out simulations with the smaller number of particles ($N = 345$).

A single run at 6000 K on our Silicon Graphics Indy workstation took approximately 10 h to complete with 345 particles, compared with several days run time for systems with 1500 particles.

Acknowledgment. The authors wish to thank Brent Poe and Peter Poole for their many helpful discussions during the course of this study as well as their many additions and improvements which were made to the molecular dynamics program. This work was supported by NSF award EAR-9219504 to P. F. McMillan.

References and Notes

(1) Wolf, G. H.; McMillan, P. F. Pressure effects on silicate melt structure and properties. In *Structure, Dynamics and Properties of Silicate Melts*; Stebbins, J. F., McMillan, P. F., Dingwell, D. B., Eds.; Mineralogical Society of America: Washington, DC, 1995; Vol. 32, p 616.

(2) Stebbins, J. F.; Farnan, I.; Xue, X. *Chem. Geol.* **1992**, *96*, 371−385.

(3) Fiske, P. S.; Stebbins, J. F. *Am. Mineral.* **1994**, *79*, 848−861.

(4) Xue, X.; Stebbins, J. F.; Kanzaki, M.; Trønnes, R. G. *Science* **1989**, *245*, 962−964.

(5) Angell, C. A.; Cheeseman, P. A.; Tamaddon, S. *Science* **1982**, *218*, 885−887.

(6) Angell, C. A.; Cheeseman, P. A.; Tamaddon, S. *Bull. Mineral.* **1983**, *106*, 87−97.

(7) Kushiro, I. *J. Geophys. Res.* **1976**, *81*, 6347−6350.

(8) Kushiro, I. *Earth Planet. Sci. Lett.* **1978**, *41*, 87−90.

(9) Kushiro, I. *Geochim. Cosmochim. Acta* **1983**, *47*, 1415−1422.

(10) Scarfe, C. M.; Mysen, B. O.; Virgo, D. Pressure dependence of the viscosity of silicate melts. In *Magmatic Processes: Physicochemical Principles*; Mysen, B. O., Ed.; The Geochemical Society: University Park, PA, 1987; pp 59−68.

(11) Kushiro, I.; Yoder, H. S., Jr.; Mysen, B. O. *J. Geophys. Res.* **1976**, *81*, 6351−6356.

(12) Wolf, G. H.; Durben, D. J.; McMillan, P. F. *J. Chem. Phys.* **1990**, *93*, 2280−2288.

(13) Xue, X.; Stebbins, J.; Kanzaki, M.; Poe, B. T.; McMillan, P. F. *Am. Mineral.* **1991**, *76*, 8−26.

(14) Stebbins, J. F.; McMillan, P. F. *Am. Mineral.* **1989**, *74*, 965−968.

(15) Stebbins, J. F. Dynamics and structure of silicate and oxide melts: Nuclear magnetic resonance studies. In *Structure, Dynamics and Properties of Silicate Melts*; Stebbins, J. F., McMillan, P. F., Dingwell, D. B., Eds.; Mineralogical Society of America: Washington, DC, 1995; Vol. 32, p 616.

(16) Poole, P. H.; McMillan, P. F.; Wolf, G. H. Computer simulations of silicate melts. In *Structure, Dynamics and Properties of Silicate Melts*; Stebbins, J. F., McMillan, P. F., Dingwell, D. B., Eds.; Mineralogical Society of America: Washington, DC, 1995; Vol. 32, pp 563−616.

(17) Farnan, I.; Stebbins, J. F. *Science* **1994**, *265*, 1206−1209.

(18) Stein, D. J.; Spera, F. J. *Am. Mineral.* **1995**, *80*, 417−431.

(19) Kubicki, J. D.; Lasaga, A. C. *Am. Mineral.* **1988**, *73*, 941−955.

(20) Woodcock, L. V.; Angell, C. A.; Cheeseman, P. *J. Chem. Phys.* **1976**, *65*, 1565−1577.

(21) Brawer, S. Relaxation in viscous liquids and glasses. In *J. Am. Ceram. Soc.* **1985**, 220.

(22) Angell, C. A.; Cheeseman, P. A.; Kadiyala, R. *Chem. Geol.* **1987**, *62*, 83−92.

(23) Rubie, D. C.; Ross II, C. R.; Carroll, M. R.; Elphick, S. C. *Am. Mineral.* **1993**, *78*, 574−582.

(24) Poe, B. T.; McMillan, P. F.; Rubie, D. C.; Chakraborty, S.; Yarger, J.; Diefenbacher, J. *Science* **1997**, *276*, 1245−1248.

(25) Rustad, J. R.; Yuen, D. A.; Spera, F. J. *Phys. Rev. A* **1990**, *42*, 2081−2089.

(26) Scamehorn, C. A.; Angell, C. A. *Geochim. Cosmochim. Acta* **1991**, *55*, 721−730.

(27) Anderson, O. L. *Equations of State of Solids for Geophysics and Ceramic Science*; Oxford University Press: New York, 1995; Vol. 31.

(28) Bottinga, Y. *Earth Planet. Sci. Lett.* **1985**, *74*, 350−360.

(29) Lange, R. L.; Carmichael, I. S. E. Thermodynamic properties of silicate liquids with emphasis on density, thermal expansion and compressibility. In *Modern Methods of Igneous Petrology: Understanding Magmatic Processes*; Nicholls, J., Russell, J. K., Eds.; Mineralogical Society of America: Washington, DC, 1990; Vol. 24, pp 25−63.

(30) Alidibirov, M.; Dingwell, D. B. *Nature* **1996**, *380*, 146−148.

(31) Brawer, S. A. *J. Chem. Phys.* **1981**, *75*, 3522−3541.

(32) Stebbins, J. F. *Nature* **1991**, *351*, 638−639.

(33) McMillan, P. F.; Wolf, G. H. Vibrational spectroscopy of silicate liquids. In *Structure, Dynamics and Properties of Silicate Melts*; Stebbins, J. F., McMillan, P. F., Dingwell, D. B., Eds.; Mineralogical Society of America: Washington, DC, 1995; Vol. 32, pp 247−315.

(34) Dingwell, D. B.; Webb, S. L. *Eur. J. Mineral.* **1990**, *2*, 427−449.

(35) Webb, S. L.; Dingwell, D. B. Viscoelasticity. In *Structure, Dynamics and Properties of Silicate Melts*; Stebbins, J. F., McMillan, P. F., Dingwell, D. B., Eds.; Mineralogical Society of America: Washington, DC, 1995; Vol. 32, p 616.

(36) Knoche, R.; Dingwell, D. B.; Seifert, F. A.; Webb, S. L. *Chem. Geol.* **1994**, *116*, 1−16.